MODELING THE BEHAVIOR OF ALUMINA AGGLOMERATE
IN THE HALL-HÉROULT PROCESS

Véronique Dassylva-Raymond[1], Laszlo I. Kiss[1], Sandor Poncsak[1], Patrice Chartrand[2], Jean-François Bilodeau[3], Sébastien Guérard[3]

[1] Université du Québec à Chicoutimi, 555 boul. de l'Université, Chicoutimi, Québec G7H2B1, Canada

[2] École Polytechnique de Montréal, 2900 boul. Édouard-Montpetit, Montréal, Québec H3C 3A7, Canada

[3] Rio Tinto Alcan - Arvida Research & Development Centre, 1955, boul. Mellon Édifice 110, Québec G7S 4K8, Canada

Keywords: alumina agglomerate, electrolyte, freeze, rapid solidification, porous media, alumina dissolution, liquid and gas infiltration

Abstract

During the feeding of the Hall-Héroult cell, cold alumina comes into contact with the electrolyte bath and tends to agglomerate due to the formation of a frozen bath layer that holds physically the alumina together. This agglomeration, producing alumina agglomerates, called also lumps or sludge, affects both the rate of alumina dissolution and the stability of the cell. In this paper, all the physical phenomena (heat and mass transfer) between the formation and the complete dissolution of agglomerate will be described and are defined by a set of equations. This mathematical model allows observing the strong coupling between the mechanisms of heat and mass transfer e.g. the solidification with diffusion of chemical species, the infiltration of the bath in the porous agglomerate and the dissolution of sintered alumina. A parametric study using this model might identify the most important factors related to the lifespan and behavior of alumina agglomerates.

Introduction

The dispersion and the dissolution of alumina in the electrolytic bath are critical steps for a good Hall-Héroult cells operation. Proper alumina feeding strategy can provide high rate of dissolution by dispersing loose alumina powder at different positions in the cell. In modern cells, alumina is injected periodically in small amounts, typically 0,5 to 2 kg per minute by 2 to 5 feeders. In addition to feeding strategy, the dispersion of alumina is also influenced by the convection in the electrolyte bath and by the tendency of alumina to form agglomerates.

The formation of alumina agglomerates affects both the rate of alumina dissolution and the stability of the cell. The dissolution behavior of alumina grains and alumina agglomerates is significantly different; the rate of agglomerate dissolution can be slower by several orders of magnitude than loose alumina. The most negative aspect related to the formation of agglomerate is the ability to form sludge on the carbon cathode. Sludge affects the velocity profile and the electric field in liquid aluminum, which create operating disturbances and losses of current efficiency.

Despite these negative aspects, the mechanism of agglomeration is essential to the Hall-Héroult process because it allows the formation of the top cover crust. Crust results from the agglomeration of alumina on the surface of the electrolytic bath and plays various important roles in the process. In addition to reducing heat loss on top of the cell, the crust protects the anodes from oxidation, minimizes splashes of cyolitic melt and limits the gas evacuation.

The objective of this study is to develop a mathematical model for the formation of alumina agglomerate. In addition to contributing to the general understanding on alumina agglomerate, the model will allow to obtain a simplified relationship that links the alumina agglomerate mass to the parameters of the process.

$$m_{ag}(t) = m_0(X_1, X_2, \dots) \cdot f(Y_1, Y_2, \dots) \qquad (1)$$

The Y_i and X_i parameters affect respectively the lifetime of the global agglomerate and the initial agglomerate mass such as feeding strategy, bath condition, alumina properties. The original mass m_0 is defined as the quantity of alumina enclosed by the frozen shell.

Background

There are a number of publications in public literature that present studies on alumina dissolution but only a few focus specifically on the formation of agglomerates. The research works of Walker [1], Kobbeltvedt et al [2] and Østbø [3] are essentially the three most significant studies concerning this topic. Rolseth and Thonstad [4] describe the formation of aggregates as a combination of the formation of a frozen shell and the γ→α alumina transformation. This frozen shell traps the alumina grains and thus keeps them physically together, while the transformation γ→α creates an interlocking network of alumina. Østbø [3] concluded that the mechanism of agglomeration is largely related to the evolution of alumina microstructure caused by the sintering in the presence of cryolithe melt, of the rapid grain coarsening and of recrystallization during change of the metastable phase γ in the stable phase α (corundum).

When the cold alumina (150-200˚C before injection) comes into contact with the electrolytic bath, a frozen layer is formed around floating or sank alumina mass. The frozen electrolyte layer, called freeze, reaches a maximum thickness after a few seconds and melts gradually due to the strong convection provoked by the motion of bubbles and the magnetohydrodynamics effect. According to Walker [1] and Kovebbelt et al [2], the formation and the melting of the frozen shell are the two longest stages controlled by heat transfer of the agglomerate lifetime. However, Taylor [5] specifies that the behavior of the alumina agglomerate smaller than 400 μm of diameter is governed by mass transfer.

The experiments of Walker [1] have shown that the first infiltration of the agglomerate by liquid bath took place even in the presence of the frozen shell. During the melting of the freeze, a thin layer of liquid electrolyte is in contact directly with alumina powder and infiltrates the pores of the agglomerate. Gradually as the infiltration front penetrates the agglomerate, it resolidifies on the coldest internal grains and melts back when the alumina

reached the local liquidus temperature of infiltrated bath. After the complete melting of the frozen shell, a second front of liquid electrolyte with the bath composition completely infiltrates the agglomerate that eventually decays.

Walker [1] studied experimentally the progress of these two fronts of infiltration by immersing cylindrical agglomerates of 6.5 centimeter of diameter in an industrial electrolytic bath. The results of Walker [1] presented in figure 1 were obtained by removing agglomerates from electrolytic bath after a given immersion time.
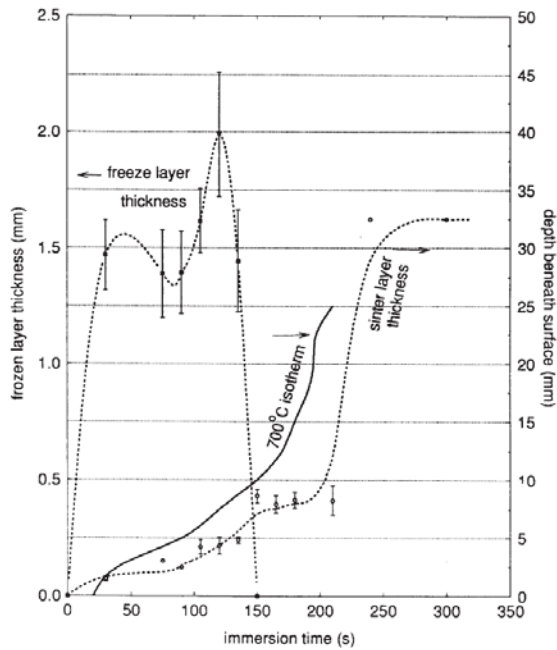
Figure 1. Freeze thickness and sinter layer evolution, Walker [1]

These experiments show clearly that the liquid bath infiltration starts long before the complete melting of the freeze. The author has added the 700°C isotherm, which corresponds to the eutectic temperature of the electrolyte, in order to demonstrate that the infiltration is a heat transfer controlled process. Indeed, the thickness of the infiltrated layer also called sinter layer by Waller [1], is approximately parallel to the 700°C isotherm.

The first infiltration contains more AlF_3 and has a lower liquidus temperature, while the other is richer in Na_3AlF_6. The second infiltration, which is not shown in figure 1, roughly follows the isotherm of 900°C. The chemical composition of each layer, 1) pure cryolite, 2) freeze, 3) and 4) the second and first infiltration layer respectively, were showed in the figure 2.

The chemical composition of the first infiltration layer is close to the eutectic composition due to two different phenomena, the AlF_3 segregation at the moving interface during the solidification and the formation of paths for liquid transport between the Na_3AlF_6 crystals in the freeze toward the agglomerate when the temperature rises above the eutectic temperature ($T_{eutectic} = 695°C$). The first liquid infiltration which has a high content of AlF_3, has a catalytic effect on the alumina $\gamma \rightarrow \alpha$ transition.

(a)

(b)
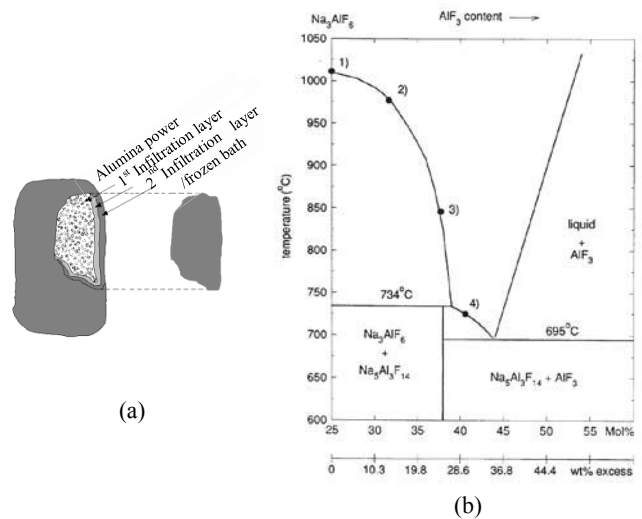
Figure 2. (a) Agglomerate formed experimentally, Østbø [3], (b) Na_3AlF_6-AlF_3 phase diagramme with the different layers, Walker [1]

According to several authors such as Rolseth and Thonstad [4], Østbø [3] and Kobbeltvedt et al [2] the polymorphic $\gamma \rightarrow \alpha$ phase transition of alumina plays a crucial role in the agglomeration mechanism. Kobbeltvedt's studies [2] demonstrated that it was not possible to form geometrically stable agglomerate from α alumina. According to Townsend and Boxall [6] and Østbø [3], an interlinking network of alumina (platelets) is created during the transformation $\gamma \rightarrow \alpha$ in the presence of cryolitic melt. The presence of platelets facilitates the liquid infiltration through the agglomerate structure and increases the mechanical strength.

A number of papers such as Hovland et al [7], Haverkamp and Welch [8] present dissolution models for individual alumina grains but there is not in the open literature a complete mathematical model dealing with the alumina agglomerate. Walker [1] has developed a numerical model using the finite volume method to predict the evolution of freeze around cylindrical and spherical agglomerate.

It is generally accepted that the alumina feeding strategy and the alumina moisture content are the parameters that affect the most the initial agglomerate size. Violent desorption of alumina moisture increases the dispersion of the alumina on the surface of the bath which reduces the risk of agglomeration.

Alumina Agglomeration Model

An alumina agglomeration model including the different phenomena between the first contact between the alumina with the electrolytic bath to the complete agglomerate dissolution is presented in this paper. The mathematical model can be divided into 5 steps or physical phenomena.

1. Moisture evolution model
2. Solidification/melting model with mass diffusion
3. Liquid and gas infiltration
4. Alumina sintering and agglomerate porosity evolution
5. Dissolution model

The mathematical model was developed two different types of agglomerates. The first represents a mass of alumina powder

604

enclosed by a layer of frozen electrolytic bath which is completely immersed in the bath. The second type is an alumina layer floating on the surface of the bath called floating "rafts".

(a)   (b)
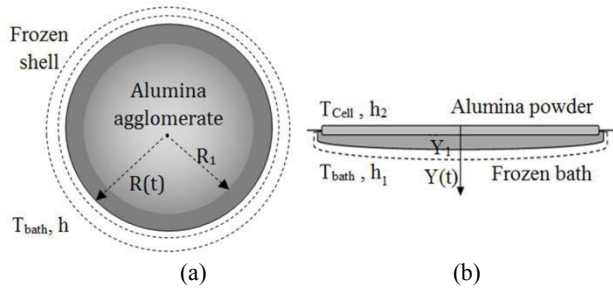
Figure 3. Schematic representation of agglomerate, (a) Spherical alumina agglomerate and (b) Floating "rafts"

The mathematical model was developed in one dimension for the spherical and planar coordinate. The governing equations used in the alumina agglomerate model are presented below:

Equation of energy

Cartesian coordinates, 1D   Spherical coordinates, 1D

$$\frac{\partial T}{\partial t} = \alpha \left(\frac{\partial^2 T}{\partial x^2} + \frac{1}{k}\dot{g} \right) \qquad \frac{\partial T}{\partial t} = \alpha \left(\frac{1}{r^2}\frac{\partial}{\partial r}\left(r^2 \frac{\partial T}{\partial r} \right) + \frac{1}{k}\dot{g} \right) \qquad (2)$$

Equation of continuity

Cartesian coordinates, 1D   Spherical coordinates, 1D

$$\frac{\partial \omega_i}{\partial t} = D_{ij}\left(\frac{\partial^2 \omega_i}{\partial x^2} \right) + \frac{\dot{r}_i}{\rho} \qquad \frac{\partial \omega_i}{\partial t} = D_{ij}\left(\frac{1}{r^2}\frac{\partial}{\partial r}\left(r^2 \frac{\partial \omega_i}{\partial r} \right) \right) + \frac{\dot{r}_i}{\rho} \qquad (3)$$

The model uses mainly second order boundary conditions, a heat transfer coefficient varying between 700-3000 W/(m$^2 \cdot$ K) and a mass transfer coefficient varying between $1\text{-}5 \cdot 10^{-3}$ m/s at the freeze-bath or agglomerate-bath moving interface. The coefficient of diffusion for alumina used in this study is equal to $1 \cdot 10^{-9}$ m^2/s.

Moisture evolution model

Alumina moisture can greatly affects the initial stage of agglomeration mechanism and have a positive impact on the alumina dissolution. The explosive desorption reduces the initial size of the aggregates but also contributes greatly to the homogenization of the internal temperature. Moisture will be investigated in two different models, the first one with a constant volume and a second model permitting the evacuation of gas at the alumina-freeze (frozen layer) interface. The volume constant model will give the increase of the agglomerate internal pressure, a parameter that can be subsequently connected to the initial agglomerate size.

In the mathematical model, alumina moisture is present as physisorbed water (H_2O) and the trihydrate ($Al_2O_3(3H_2O)$). The initial moisture quantity corresponds to the humidity (0-100°C) parameter for the H_2O and to the M.O.I. (110-300°C) and the L.O.I. (300-1000°C) for the $Al_2O_3(3H_2O)$. The transition of alumina trihydrate (gibbsite) through the monohydrate (boemite), to corundum is outlined according Llavona et al [9] as follows:

$$Al_2O_3 \cdot (3H_2O) \xrightarrow{320°C} Al_2O_3 \cdot H_2O + 2H_2O_{(g)} \qquad (4)$$

$$Al_2O_3 \cdot H_2O \xrightarrow{550°C} Al_2O_3 + H_2O_{(g)} \qquad (5)$$
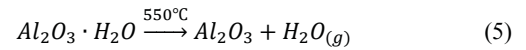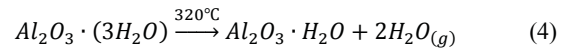
Once the water has evaporated, it can react with cryolite to produce hydrogen fluoride (HF) at freeze-alumina interface. The gas infiltration flow can be represented by the summation of Fick's law for a porous medium and Darcy's law of gas filtration.

$$\vec{J_v} = -\rho_v \frac{P_g}{P_v} D_v \vec{\nabla}\left(\frac{P_v}{P_g} \right) - \rho_v \frac{K \kappa_g}{\mu_g} \vec{\nabla} P_g \qquad (6)$$

where the indices v and g are respectively the vapor and gas mixture. The intrinsic permeability of the porous medium can be approximated by the following relation:

$$K = 0.2\varepsilon \left[\frac{\varepsilon}{A(1-\varepsilon)} \right] \qquad (7)$$

where ε is the porosity and A is specific surface, two parameters that will evolve with time according to different physical phenomena. Gas production contributes to the homogenization of the temperature through evaporation and condensation cycles. The heat flux generated by the phase change is added to the heat flux by conduction.

$$\vec{q} = -k\vec{\nabla}T + L \vec{J_v} \qquad (8)$$

To study the evolution of the internal pressure in spherical agglomerate, an independent model using a constant agglomerate volume was first developed. The first hypothetical model was used to observe the evolution of the average internal pressure of the agglomerate. The model showed that the evaporation of a 1 wt% of moisture increases the initial pressure of 70 times higher.

An experimental study on the cryolitic melt solidification in a laboratory cell, it was possible to observe that a few millimeters thick of freeze was cracking under the effect of thermal expansion. The low mechanical resistance of the solidified bath is suggesting that the freeze layer cracks in one or more places under the increase of pressure caused by gas formation as presented in figure 4. To represent the mass flow of gas evacuation in the mathematical model, a constant pressure corresponding to the hydrostatic pressure of the bath is applied to the freeze-bath interface.
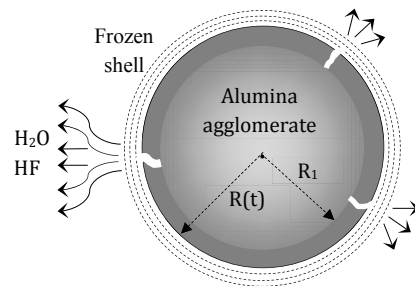
Figure 4. Shematic represntation of gas evacuation through carcks on the freeze surface for spherical agglomerate

Solidification/melting model with mass diffusion

The consecutive formation and melting of the frozen shell, as the longest step controlled by the heat transfer of agglomerate

605

lifetime, have a crucial impact on the agglomeration mechanism. Indeed, the presence of a concentration gradient in the frozen shell and the melting of this last one at the liquidus temperature are the origin of the first infiltration front.

Chemical composition of the freeze depends both on the temperature of solidification and the growth rate. The rate of freeze solidification is initially high, but decreases gradually until reaching the maximum freeze thickness. For low growth rate ($v_i \approx 0\ m/s$), the chemical potentials at the interface equalize and the system become in thermodynamic equilibrium that allows mass diffusion of the solute at the solid/liquid interface. In contrast, if the solidification rate is larger than the rate of diffusion over an interatomic distance ($v_i \geq D_{ij}/\delta_i$) this results in a loss of equilibrium interface and leads to a complete solute trapping.

To obtain the concentration of the solute in each phase for the two types of solidification e.i. with and without mass diffusion, the mathematical model used the Aziz [10] relationships. The non-equilibrium distribution coefficient is a function of the rate of interfacial movement and it is used to calculate the rejected mass of solute.

$$k(v) = \frac{C_s}{C_l} = \frac{k_e(T, wt\%) + P_i}{1 + P_i} \quad \text{if } P_i = (v_i \delta_i / D_{ij}) < 1 \quad (9)$$

$$k(v) = 1 \quad \text{if } P_i = (v_i \delta_i / D_{ij}) \geq 1 \quad (10)$$

where $P_i = v_i \delta_i / D_{ij}$ is the interface Peclet number and D_{ij}/δ_i is the maximum speed which the diffusion at the interface is possible. The partition coefficient at equilibrium can be determined with the initial bath composition using the thermochemical software FactSage® which used a specific database for alumina reduction electrolysis cells.

Liquid and gas infiltration

In addition to the infiltration of liquid bath, Walker [1] mentioned the possibility of a first infiltration by bath in a gaseous form. The most likely vaporization reaction would be as follows:

$$Na_3AlF_{6(s)} \rightarrow NaAlF_{4(g)} + 2NaF_{(s)} \quad (11)$$
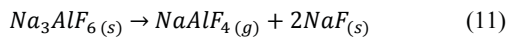
For temperatures between 850 and 950C°, the vapor pressure of the $NaAlF_4$ is between 0.002-0.005 atm. The $NaAlF_4$ gas flow is calculated by the relation 10. Infiltration of liquid electrolyte in alumina agglomerate will be treated using Darcy's infiltration law.

$$\vec{J_l} = \rho_l \frac{K}{\mu_l} \vec{\nabla} P_l \quad (12)$$

The thermal contribution of liquid and gas infiltration will be treated the same way as the evaporation/condensation cycles of the moisture evolution model. Energy related to the internal solidification or condensation of the bath infiltration will be added to the Fourier's law in the heat flux, whereas the fusion or evaporation enthalpy is processed by the enthalpy method.

Alumina sintering and agglomerate porosity evolution

The mechanism of alumina sintering is mainly caused by two phenomena, grain coarsening and formation of alumina platelets

which are produced during the γ→α phase transition in the presence of liquid fluoride. In the mathematical model, the phase change of the alumina occurs instantaneously in the entire agglomerate volume and the first contact between alumina and liquid bath (first infiltration) has been selected as triggering criterion.

The agglomerate porosity (void fraction) varies in space and time and can be obtained by the following equation:

$$\varepsilon(r, t) = 1 - \frac{\rho_{bulk}(r, t)}{\rho_{particle}} \quad (13)$$

The bulk density is affected by various phenomena such as infiltration by the liquid bath, vapor condensation between alumina pores, thermal expansion and sintering of alumina. Impacts of the two first phenomena on the porosity are considered in the calculation of density of each element for each time step in the mass conservation module. The model also uses published empirical relationships to account for the thermal expansion of the alumina powder.

Dissolution and disintegration model

The dissolution of agglomerate starts during the first liquid infiltration. Liquid bath rich in AlF_3 that slowly penetrate agglomerate becomes quickly saturated in alumina. For this phenomenon, the model considers that each element is in thermochemical equilibrium. The heat of dissolution is represented numerically by enthalpy method.

The dissolution of agglomerate after the complete melting of the frozen shell is likely a mechanism under mass control due to the small contact area between the alumina and bath. The mass flow of dissolved alumina at the agglomerate-bath interface may be calculated by the following relation:

$$-D_{Al_2O_3/bath} \frac{\partial \omega_{Al_2O_3}}{\partial r}\bigg|_{r=R(t)} = h_{mass} \left(\omega_{Al_2O_3} - \omega_{sat_{Al_2O_3}} \right) \quad (14)$$

The heat mass coefficient can be obtained from the Chilton-Colburn [11] analogies.

$$h_{mass} = \frac{h_{conv}}{\rho c_p} \left(\frac{\alpha}{D_{ij}} \right)^n \quad (15)$$

where n = 1/3. The maximal alumina solubility can be calculated with the chemical composition of the bath using the empirical relation of Skybakmoen et al [12].

Numerical Method

The mathematical model using the finite difference method is developed in MathLab®. Simple explicit method was preferred to the Crank-Nicolson method because of the many non-linear relations. The numerical model is developed with a fixed grid discretization model and used central difference approximations.

The software MatLab® was selected for solving the heat and mass balance equations as well as for the calculations of the various submodel such as the alumina and bath properties, alumina porosity evolution and calculations of the gas and liquid infiltration flows. For phenomena that can assume the hypothesis

of a local thermodynamic equilibrium, thermodynamic data was obtained by the software FactSage®.

To represent the phase change of the bath, the alumina dissolution and chemical reactions related to the alumina moisture content, the thermal model uses enthalpy method as mentioned above. The energy associated to chemical reactions that occur locally like the HF production on the inner surface of the freeze is introduced into the source terms. The energy related to the transition of alumina $\gamma \rightarrow \alpha$ will also be included in the internal heat generation term due to the instantaneous reaction speed.

Results

An overview of the results obtained with the alumina agglomerate model is presented in this section. Figures 5 and 6 show the results of simulation for an agglomerate with a diameter of 30 mm immersed in a bath at 975°C with a superheat of 15°C.
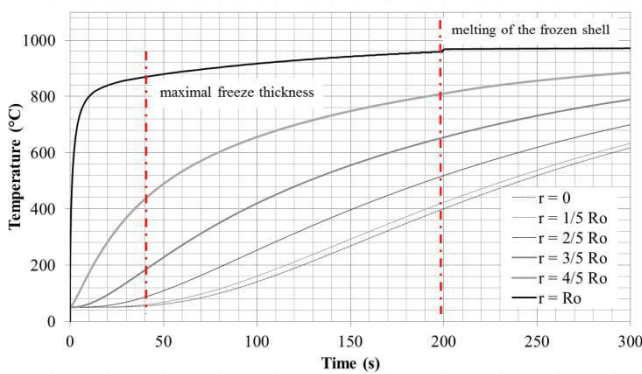
Figure 5. Internal temperature profile of a spherical of 30 mm of diameter

Figure 5 shows the evolution of temperature at different positions inside alumina agglomerate. It can be seen the sudden increase of temperature at the agglomerate surface around 200 secondes that corresponds to the complet melting of the frozen shell. Examples of evolution of freeze thickness and AlF_3 concentration at the solid-liquid interface are presented in figure 6.
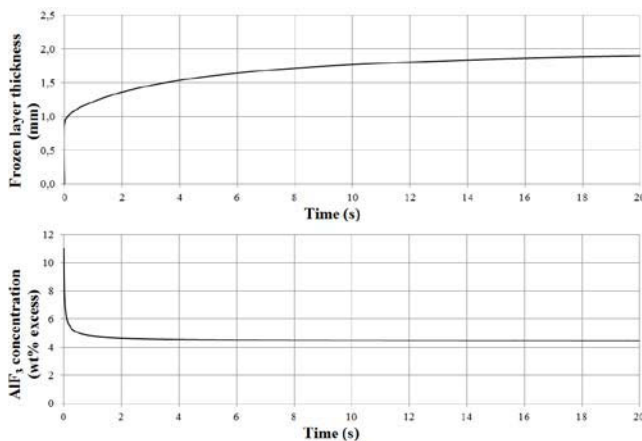
Figure 6. Evolution of freeze thickness and AlF_3 concentration for spherical agglomerate of 30 mm of diameter

Results from the mathematical model were also compared with experimental studies of Walker [1] on cylindrical shaped agglomerates immersed in experimental and industrial cells. For these simulations, the coordinates of the model was modified into cylindrical coordinates and the same conditions as mentioned in Walker [1] were employed.
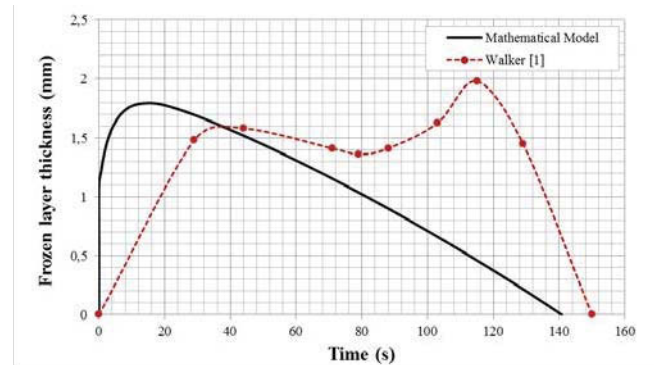
Figure 7. Comparaison of the frozen layer thickness for a cylindrical agglomerate of 65 mm of diameter

The mathematical model was able to estimate correctly the lifetime and the maximal frozen thickness but differs slightly for the shape of the curve of the freeze thickness evolution as show in figure 7.
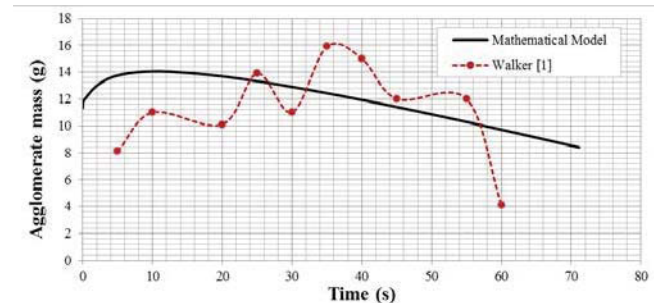
Figure 8. Comparaison of agglomerate mass for a cylindrical shaped agglomerate of 15 mm of diameter

The differences between the model and the experimental studies may be can be due to the fact that a 1D model cannot represent correctly the effect of the flow variation along the agglomerate.

Conclusion

A mathematical model descried the behavior of alumina agglomerate has been developed. This model includes the various mechanisms of heat and mass transfer taking place between the first contact of the alumina powder on the cryolitic melt until the complete agglomerate dissolution. The mathematical model of the formation of alumina agglomerate was solved numerically using the software Matlab® by a finite difference method.

The preliminary simulations permitted to obtain the evolution of the thickness and chemical composition of the freeze as well as agglomerate mass and were partially compared to the experimental results of Walker [1]. In the near future a complete parametric study will be made in order to evaluate the sensitivity of the alumina agglomerate model presented in this paper.

607

Nomenclature

A	Specific surface, m^2/m^3
C_l	Concentration of solute in liquid part, wt%
C_s	Concentration of solute in solid part, wt%
D_{ij}	Coefficient of diffusion, m^2/s
$\vec{q}$	Heat flux, W/m^2
h_{conv}	Heat transfer coefficient, $W/(m^2 \cdot K)$
h_{mass}	Mass transfer coefficient, m/s
$\vec{J}$	Mass flow, kg/m^2
K	Intrinsic permeability
k	Thermal conductivity, $W/(m \cdot K)$
k_e	Equilibrium coefficient partition
k_{ne}	Non-equilibrium coefficient partition
L	Latent heat, J/kg
m	Mass, kg
v_i	Interfacial velocity, m/s
α	Thermal diffusivity, m^2/s
δ_i	Intermolecular distance, m
ε	Porosity (void fraction)
κ	Relative permeability
μ	Dynamic viscosity, Pa·s
ρ	Density, kg/m^3

References

1. David I. Walker, "Alumina in aluminium smelting et its behaviour after addition to cryolite-based electrolytes", PhD thesis (1993), University of Toronto.

2. O. Kobbeltvedt, S. Rolseth and J. Thonstad, "On the mechanism of alumina dissolution with relevance to point feeding aluminium cells", *Light Metals* (1996), 421-427.

3. Peter Østbø, "Evolution of alpha phase alumina in agglomerates unpon addition to cryolitic melts", Phd Thesis, Norwegian University of Science and Technology (2002).

4. S. Rolseth and J. Thonstad, "Agglomeration and dissolution of alumina", *Proc. of the Intl. Symp. on Extraction, Refining and Fabrication of Light Metals*, Ottawa, Ontario, Canada (1991) 177-190.

5. M. P. Taylor, B. J. Welch, S. Rolseth, J. Thonstad, "On alumina phase change on the stability of aluminium smelting cells", *Journal of A.I.Ch.E*, Vol. 32 (1986), 1459-1465.

6. D.W. Townsend and L.G. Boxall. "Crusting behaviour of smelter alumina", *Light Metals* (1984), 649-665.

7. R. Hovland, S. Rolseth, and A. Solheim. "On the alumina dissolution in cryolitic melts". *Proc. of the Intl. Symp. on Light Metals Processing and Applications, Quebec*, Canada(1993), 3-16.

8. R.G. Haverkamp and B.J.Welch, "Modelling the dissolution of alumina powder in cryolite", *Chem. Eng. Processing 37* (1998), 177-187.

9. M. A. Llavona, F. Blanco, P. Garcia, J. Sancho, and L. F. Verdeja, "Some new considerations on the measurement of humidity, M.O.I. and L.O.I. ", *Light Metals* (1988).

10. M. J. Aziz, "Non-equilibrium interface kinetics during rapid solidification: theory and experiment", *Materials Science and Engineering*, 98 (1988), 369-372.

11. R.B. Bird, W.E. Steward, and E.N. Lightfoot. "Transport Phenomena", John Wiley & Sons Inc., New York, NY, 1960.

12. E. Skybakmoen, A. Solheim and A. Sterten, "Alumina Solubility in Molten Salt Systems of Interest for Alumina Electrolysis and Related Phase Diagram Data", *Met. Mat. Trans. B.*, 28B, 81-86, 1997.

13. E. Patterson, "Hydrogen fluoride emissions from aluminium electrolysis cells", PhD thesis (2001), The Universityof Auckland.

14. D.I. Walker, T.A. Utigard and M. P. Taylor, "Alumina agglomerates in aluminium smelters", *Ligth Metal* (1995), 425-434

15. J. Gerlach and G. Winkhaus, "Interactions of alumina with cryolite based melts", *Light Metals* (1985), 301-313.

16. James B. Metson, Margaret M. Hyland and Tanya Groutso, "Alumina properties and impacts on emissions from reduction cells", *Proc. 8th Aust. Al Smelting technology conference and workshop*, (2004), 1-8.

17. T.J. Johnston and N.E. Richards, "Correlation between alumina and properties of crust", *Light Metals* (1983), 623-639.

18. J. Thonstad, A. Solheim, S. Rolseth, and O. Skar, "The dissolution of alumina in cryolite melts", *Light Metals* (1988), pages 655-660.